The Journal of Immunology

IRAK1 Limits TLR3/4- and IFNAR-Driven IL-27 Production through a STAT1-Dependent Mechanism

Daniela Bruni, Adam Dignam, Susan Dunne, Devlin Wall-Coughlan, Aisling McCrudden, Karen O'Connell, Caitriona Lyons, Christopher McGuigan, Niall Tubridy and Marion P. Butler

J Immunol 2018; 201:2070-2081; Prepublished online 24 August 2018;
doi: 10.4049/jimmunol.1701373
http://www.jimmunol.org/content/201/7/2070

The Journal of Immunology is published twice each month by
The American Association of Immunologists, Inc.,
1451 Rockville Pike, Suite 650, Rockville, MD 20852

Print ISSN: 0022-1767 Online ISSN: 1550-6606.

IRAK1 Limits TLR3/4- and IFNAR-Driven IL-27 Production through a STAT1-Dependent Mechanism

Daniela Bruni,*,[1] Adam Dignam,*,[1] Susan Dunne,*,[1] Devlin Wall-Coughlan,* Aisling McCrudden,* Karen O'Connell,†,‡ Caitriona Lyons,* Christopher McGuigan,†,‡ Niall Tubridy,†,‡ and Marion P. Butler*

IL-27 is a cytokine exerting pleiotropic immunomodulatory effects on a broad spectrum of immune cells. Optimal IL-27 production downstream of TLR3/4 ligand stimulation relies on autocrine type I IFN signaling, defining a first and second phase in IL-27 production. This work shows that IL-1 receptor-associated kinase 1 (IRAK1) limits TLR3/4- and IFNAR-induced IL-27 production. At the mechanistic level, we identified IRAK1 as a novel regulator of STAT1, IRF1, and IRF9. We found hyperactivation of STAT1 together with increased nuclear levels of IRF1 and IRF9 in IRAK1-deficient murine macrophages compared with control cells following stimulation with LPS and poly(I:C). IRAK1-deficient human microglial cells showed higher basal levels of STAT1 and STAT2 compared with control cells. Blocking the kinase activity of TBK1/IKKε in IRAK1 knockdown human microglial cells reduced the high basal levels of STAT1/2, uncovering a TBK1/IKKε kinase–dependent mechanism controlling basal levels of STAT1/2. Stimulating IRAK1 knockdown human microglial cells with IFN-β led to increased IL-27p28 expression compared with control cells. In IRAK1-deficient murine macrophages, increased IL-27 levels were detected by ELISA following IFN-β stimulation compared with control macrophages together with increased nuclear levels of p-STAT1, IRF1, and IRF9. Treatment of wild-type and IRAK1-deficient murine macrophages with fludarabine similarly reduced TLR3/4-induced IL-27 cytokine levels. To our knowledge, this work represents the first report placing IRAK1 in the IFNAR pathway and identifies IRAK1 as an important regulator of STAT1, controlling IL-27 production downstream of TLR3/4 and IFNAR signaling pathways. ***The Journal of Immunology*****, 2018, 201: 2070–2081.**

Interleukin 27 is a heterodimeric cytokine composed of the subunits EBV-induced gene 3 (EBI3) and IL-27p28 (1) and is a member of a family of cytokines that includes IL-12, IL-23, and IL-35. IL-27 is mainly produced by monocytes, macrophages, dendritic cells, and microglial cells in response to TLR3, -4, and -9 ligand stimulation (2, 3). Optimal IL-27p28 expression relies on autocrine type I IFN signaling following TLR ligand stimulation (4). IL-27 binds to a heterodimeric cell surface receptor that consists of two subunits: gp130, which belongs to the IL-6 family and is shared by many other cytokine receptors, and IL-27Rα (WSX1/TCCR). IL-27Rα specifically recognizes IL-27, and consequently, IL-27Rα distribution determines the cellular targets of IL-27. IL-27Rα is expressed on T cells, B cells, NK cells, neutrophils, monocytes, mast cells, and at lower levels on macrophages and endothelial cells (5). Upon IL-27 binding, IL-27R becomes activated, initiating a signaling cascade that involves several members of the JAK/STAT pathway, notably STAT1 and STAT3. IL-27 prevents the differentiation of Th2, Th17, and regulatory T cells by suppressing the corresponding master transcription factors GATA-3, ROR-γτ, and FOXP3, respectively (6–8). In contrast, IL-27 promotes Th1 polarization and synergizes with IL-12 in the production of the Th1 signature cytokine IFN-γ (9, 10). IL-27 also supports the differentiation of naive $CD4^+$ T cells into the IL-10–producing T regulatory 1 cells, which are often deregulated in autoimmune diseases (11–13).

IL-27 reduces disease severity in several animal models of autoimmune diseases, including those representing multiple sclerosis (MS) and rheumatoid arthritis, through suppressing the development of pathogenic Th17 cells (14–18). Studies in rheumatoid arthritis have shown that $CD14^+$ mononuclear cells are the key cellular sources of IL-27 that infiltrate into the synovium of arthritic joints, reducing inflammation (19). Studies involving newly diagnosed and progressive MS patients showed reduced plasma/serum levels of IL-27 when compared with healthy control subjects (20–22). In progressive MS, plasma levels of IL-27 negatively correlated with both the percentages of circulating Th17 cells and plasma levels of IL-17 (20).

IL-27 also exerts antitumor activities through the upregulation of Th1, $CD8^+$ CTL, and NK cell responses, key immune cell players in mediating the antitumor immune response (23–28).

TLR-induced expression of EBI3 in dendritic cells is dependent on NF-κB and PU.1 (29). The IL-27p28 promoter has a distal

*Institute of Immunology, Department of Biology, Maynooth University, Maynooth, County Kildare, Ireland; †Department of Neurology, St. Vincent's University Hospital, Dublin 4, Ireland; and ‡School of Medicine, University College Dublin, Dublin 4, Ireland

[1]D.B., A.D., and S.D. contributed equally to this work.

ORCIDs: 0000-0003-2015-3891 (D.B.); 0000-0003-4126-2819 (A.D.); 0000-0001-6063-1590 (D.W.-C.); 0000-0002-8470-3760 (A.M.).

Received for publication September 28, 2017. Accepted for publication July 25, 2018.

This work was supported by Health Research Awards (Grants HRA-POR-2012-89 and HRA-POR-2015-1352), both of which were funded by the Irish Health Research Board (HRB). D.B. was funded by HRB Grant PHD/2007/9.

Address correspondence and reprint requests to Dr. Marion P. Butler, Institute of Immunology, Department of Biology, Maynooth University, Maynooth, County Kildare, Ireland. E-mail address: marion.butler@mu.ie

The online version of this article contains supplemental material.

Abbreviations used in this article: BMDM, bone marrow–derived macrophage; EBI3, EBV-induced gene 3; IFNAR, IFN-α receptor; ISGF3, IFN-stimulated gene factor 3; ISRE, IFN-stimulated regulatory element; mIFN-β, murine mIFN-β; MS, multiple sclerosis; qRT-PCR, quantitative RT-PCR; shRNA, short hairpin RNA; WT, wild-type.

NF-κB site as well as an IFN-stimulated regulatory element (ISRE) site. Following TLR3/4 engagement, the transcription factors IRF3 and NF-κB become activated, and both drive IL-27p28 and IFN-β gene expression (2, 30). The TLR4–MyD88-dependent pathway also leads to the activation of IRF1 (31, 32) and IRF8 (33), which bind to an ISRE in the IL-27p28 promoter, driving p28 subunit expression. Autocrine type I IFN signaling leads to a STAT1-dependent increase in IRF1 expression and sustained activation of IRF1 follows. IRF1 binds to an ISRE site in the p28 promoter. Importantly, type I IFN results in the activation of the IFN-stimulated gene factor 3 (ISGF3) (STAT1/STAT2/IRF9) complex, which is also recruited to the ISRE site in the p28 promoter, amplifying IL-27p28 gene expression (4, 34). ISGF3 also leads to IRF7 gene induction, thereby amplifying IFN-β production, which acts to positively influence IL-27p28 gene expression. TLR3 and -4 pathway-specific differences exist, including the dynamics and intensity of IL-27p28 gene activation as well as their differential dependency on IRF transcription factors mediating IL-27p28 expression (4).

This study identified IRAK1 as a pivotal signaling molecule controlling IL-27 production induced by TLR3 and -4 ligands. Optimal IL-27 production following TLR ligand stimulation relies on autocrine type I IFN signaling. Based on our mechanistic findings, we explored whether IRAK1 acts downstream of IFN-α receptor (IFNAR). Our findings place IRAK1 downstream of IFNAR, regulating the STAT1/ISGF3 signaling axis controlling IL-27 cytokine production.

Materials and Methods

Cell lines

Wild-type (WT) and IRAK1$^{-/-}$ bone marrow–derived macrophages (BMDM), TBK1$^{-/-}$TNFR1$^{-/-}$ BMDM, and the control cell line TBK1$^{+/+}$ TNFR1$^{-/-}$ BMDM were gifts from Dr. K. Fitzgerald (University of Massachusetts Medical School, Worcester, MA). The human microglial cell line CHME3 was provided by Dr. M. Naghavi (Columbia University, New York, NY).

Abs and reagents

Anti–phospho-STAT1, both Ser^{727} and Tyr^{701}, anti-IRAK1, and anti-IRF1 were purchased from Santa Cruz Biotechnology. Anti–phospho-IRF3 (Ser^{396}) and anti-IRF1 (human) were from Cell Signaling Technology. β-Actin was from Sigma-Aldrich and anti-IRF9 from R&D Systems and Cell Signaling Technology. Poly(I:C) (high molecular weight) (InvivoGen) was used at a final concentration of 25 μg/ml. LPS (Enzo Life Sciences) was used at a final concentration of 1 μg/ml. Human IFN-β (hIFN-β) (ImmunoTools) and murine IFN-β (mIFN-β) (R&D Systems) were used at a final concentration of 10 ng/ml. The dual IKKε/TBK1 kinase inhibitor MRT67307 was purchased from the Medical Research Council Protein Phosphorylation and Ubiquitylation Unit, University of Dundee and was used at a final concentration of 2 μM. Fludarabine (Sigma-Aldrich) was used at a 50-μM final concentration.

Western blot analysis

Following a time course of stimulation using poly(I:C) (25 μg/ml), LPS (1 μg/ml), or IFN-β (10 ng/ml), cells were lysed in lysis buffer containing 50 mM Tris HCl (pH 7.5), 150 mM sodium chloride, 0.5% (v/v) IGEPAL, 50 mM sodium fluoride, 1 mM sodium orthovanadate, 1 mM DTT, 1 mM PMSF, and protease inhibitor mixture (Roche). The lysates were resolved by SDS-PAGE, transferred to PVDF (GE Healthcare), and probed with the indicated Abs. Where relevant, nuclear and cytosolic fractionation was performed using the Nuclear Extract Kit (Active Motif) as per manufacturer's instructions.

Real-time PCR

Total RNA was extracted from cell cultures using TRI Reagent (Sigma-Aldrich). Total RNA was reverse transcribed to cDNA using All-In-One RT MasterMix (ABMgood) according to the manufacturer's instructions. Quantitative real-time PCR was performed on a StepOnePlus Real-Time PCR System (Applied Biosystems) using the FastStart Universal SYBR Green Master Mix (Rox) (Roche). The data were analyzed using the $2^{-\Delta\Delta Ct}$ relative method, with all samples normalized to GAPDH. All experiments were conducted in triplicate. Primer sequences used in this study for amplification of murine and human target genes are provided in Table I.

ELISA

ELISAs were used to measure the levels of murine IL-27 in the supernatant of WT and IRAK$^{-/-}$ BMDM using the Mouse IL-27 ELISA Ready-SET-Go! from eBioscience. BMDM were seeded at 1×10^6/ml and stimulated with poly(I:C) (25 μg/ml) for 9 h, LPS (1 μg/ml) for 6 h, or IFN-β for 8 h. Where specified, cells were pretreated with inhibitors, as detailed in the figure legends. CHME3 cells were seeded at 5×10^6 cells/ml and stimulated for 12 h with poly(I:C) or LPS, supernatants were collected, and the levels of IL-27 were measured by ELISA (eBioscience). All ELISAs were conducted at least in triplicate and according to the manufacturer's instructions. The average (±SEM) was calculated for at least three experiments except in the case of patients' samples.

Lentiviral knockdown

HEK293T cells were transfected using GeneJuice (Novagen) according to the manufacturer's instructions with the packaging plasmid pCMV-dR 8.91 (1 μg), envelope plasmid VSV-G (1 μg) and IRAK1 sh-pLKO.1 vector (2 μg; Sigma-Aldrich), or control short hairpin RNA (shRNA) (Sigma-Aldrich). The control shRNA was a nontargeting shRNA vector. Medium was replaced 24 h posttransfection with a 30% (v/v) FBS-containing medium for a further 24 h. The lentivirus-containing medium was harvested 24 h later, fresh medium was added, and lentiviral particles were collected again 24 h later. CHME3 cells seeded into T75 flasks were transduced with 2 ml lentivirus-containing medium with hexadimethrine bromide (8 μg/ml) and incubated for 24 h prior to adding puromycin (2 μg/ml), which positively selected cells with integrated shRNA constructs.

Statistical analysis

Data analysis was carried out using the unpaired Student *t* test: $*p < 0.05$, $**p < 0.01$, $***p < 0.001$. When data, tested using the D'Agostino–Pearson omnibus normality test, were not normally distributed, the *p* value was calculated using the Mann–Whitney *U* test. One-way ANOVA with a post hoc Tukey test was conducted for multiple experimental group comparison.

Results

Probing TLR-regulated IL-27 production reveals a novel role for IRAK1 in limiting IL-27 production downstream of TLR3 and TLR4

Measuring IL-27 levels by ELISA in poly(I:C)-treated WT and IRAK1-deficient BMDM revealed a significant increase in IL-27 production in IRAK1$^{-/-}$ macrophages [$p < 0.01$ and $p < 0.05$, 6 and 9 h of poly(I:C), respectively; Fig. 1A]. Similarly, heightened IL-27 production was observed in TLR4 ligand–stimulated, IRAK1-deficient macrophages compared with WT macrophages ($p < 0.05$, following 6 h of LPS; Fig. 1A). IRF3 has been shown to be critically involved in TLR4-induced and, to a lesser extent, TLR3-induced IL-27p28 expression (4). Given the importance of TBK1 in IRF3 activation and IFN-β production downstream of these TLRs, we next assessed whether inhibiting the kinase activity of TBK1 reduced both TLR3- and 4-induced IL-27 cytokine responses. Pretreating WT BMDM with MRT67307, a dual TBK1/IKKε kinase inhibitor, led to a significant reduction in both TLR4- and TLR3-induced IL-27 production ($p < 0.05$; Fig. 1B). We next tested whether the dual TBK1/IKKε kinase inhibitor, MRT67307, could reduce the TLR-induced hyper–IL-27 cytokine response observed in IRAK1-deficient macrophages similarly to that seen in inhibitor-treated WT macrophages. Using MRT67307, we observed significantly reduced IL-27 production in IRAK1$^{-/-}$ BMDM following LPS stimulation ($p < 0.05$), with a less pronounced reduction seen in poly(I:C) ligand–stimulated IRAK1$^{-/-}$ BMDM (Fig. 1C). This finding suggested a functional difference between the TLR3 versus TLR4 signaling pathways involving the

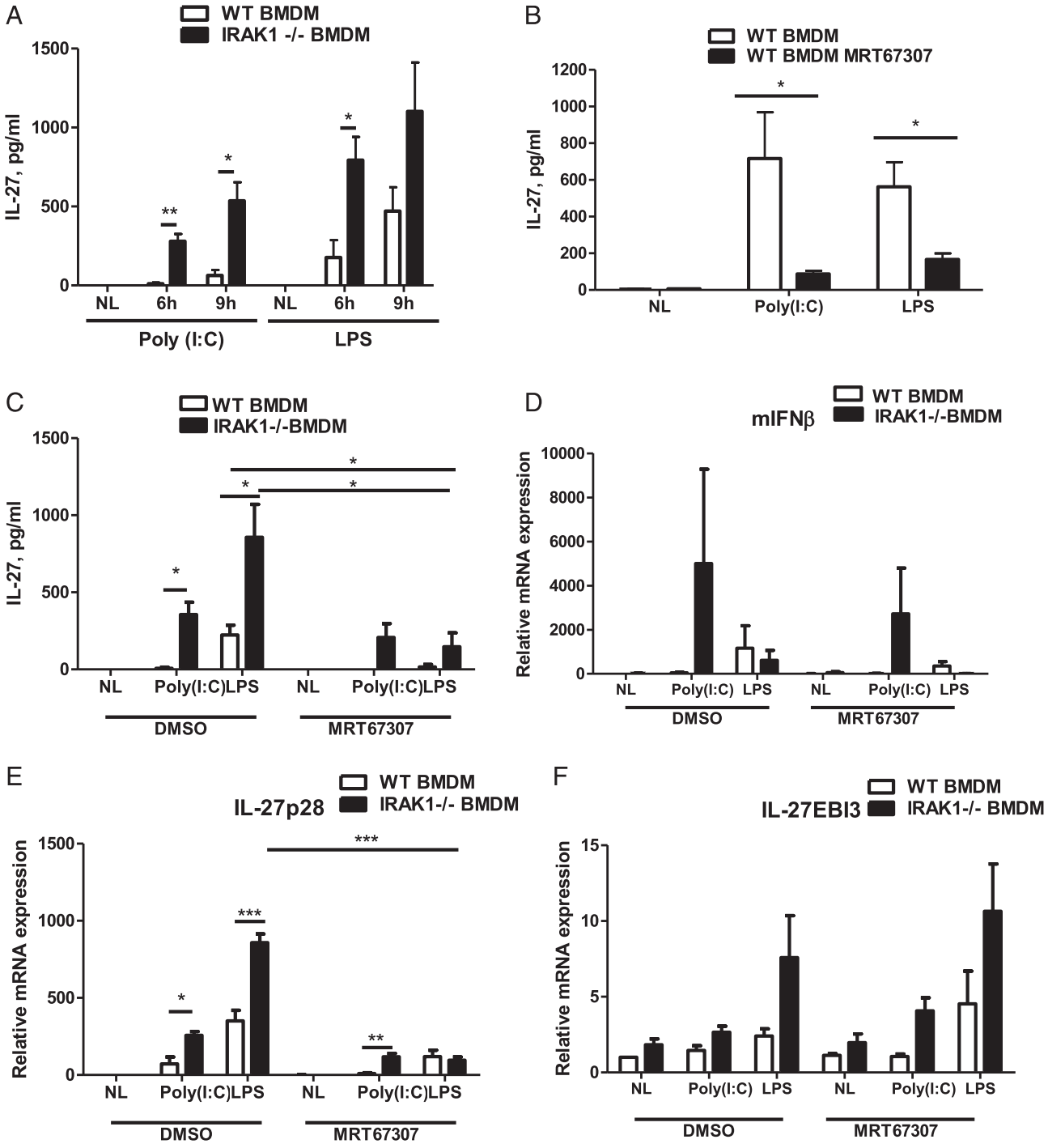

FIGURE 1. IRAK1 limits TLR3- and TLR4-driven IL-27 production, in part through TBK1-dependent mechanisms. (**A**) WT or IRAK1$^{-/-}$ BMDM were seeded and stimulated with 25 μg/ml poly(I:C) or 1 μg/ml LPS. Supernatants were collected after 6 and 9 h, and IL-27 levels were measured through ELISA. Data are the mean (±SEM) of three independent experiments performed in triplicate. The *p* values were calculated using the unpaired Student *t* test. (**B**) Kinase-active TBK1/IKKε has a major role in the regulation of IL-27 production downstream of TLR3 or TLR4. WT BMDM were seeded and stimulated for 9 h with 25 μg/ml poly(I:C) or for 6 h with 1 μg/ml LPS. Cells had been pretreated with 2 μM MRT67307 (dual TBK1/IKKε kinase inhibitor) or the same volume of DMSO as a vehicle control. Supernatants were collected, and IL-27 levels were measured by ELISA. Data shown are the mean (±SEM) of four independent experiments performed in duplicate. The data, tested using the D'Agostino–Pearson omnibus normality test, were not normally distributed, and thus the *p* value was calculated using the Mann–Whitney *U* test. (**C**) MRT67307 reduces the heightened IL-27 cytokine levels observed in IRAK1-deficient macrophages following LPS and poly(I:C) stimulation. WT and IRAK1-deficient BMDM were seeded; the next day, cells were treated with DMSO or the TBK1/IKKε kinase inhibitor MRT67307 (2 μM) for 1 h prior to poly(I:C) or LPS stimulation. After 6 h, the supernatant was collected and analyzed for IL-27 by ELISA. Data are shown as mean (±SEM) of three independent experiments. The *p* value was calculated using the unpaired Student *t* test. (**D**–**F**) IRAK1 regulates the transcription of IFN-β, IL-27p28, and EBI3. WT or IRAK1$^{-/-}$ BMDM were seeded and stimulated for 3 h with 25 μg/ml poly(I:C) or 1 μg/ml LPS. Cells had been pretreated with 2 μM MRT67307 or the same volume of DMSO as a vehicle control. Total RNA was isolated and subjected to reverse transcription. IFN-β, IL-27p28, and EBI3 mRNA was measured by quantitative real-time RT-PCR, normalized against GAPDH mRNA, and shown as the mean (±SEM) of three independent experiments performed in triplicate. One-way ANOVA with a post hoc Tukey test was conducted for multiple experimental group comparison. *$p < 0.05$, **$p < 0.01$, ***$p < 0.001$. NL, no ligand.

Table I. Primer sequences for real-time PCR

Gene	Forward	Reverse
mIL-27 p28	5′-CTC TGC TTC CTC GCT ACC AC-3′	5′-GGG GCA GCT TCT TTT CTT CT-3′
mEBI3	5′-TGA AAC AGC TCT CGT GGC TCT A-3′	5′-GCC ACG GGA TAC CGA GAA-3′
mGAPDH	5′-CCA TGC CAT CAC TGC CAC CCA GAA-3′	5′-GTC CAC CAC CCT GTT GCT GTA GCC-3′
mIRF1	5′-TCG TCA GCA GCA GTC TCT CT-3′	5′-TTC GGC TAT CTT CCC TTC CT-3′
mIRF9	5′-GTC TGG AAG ACT CGC CTA CG-3′	5′-GTG ATT TCT GGT TCC GTG GT-3′
mSTAT1	5′-AAG CGA ACT GGA TAC ATC A-3′	5′-CCG GGA CAT CTC ATC AAA C-3′
hIL-27p28	5′-GCG GAA TCT CAC CTG CCA-3′	5′-GGA AAC ATC AGG GAG CTG CTC-3′
hEBI3	5′-TAA CAG AGC ACA TCA TCA AG-3′	5′-TTG AGT GAG AAG ATC TCT GG-3′
hGAPDH	5′-ACA GTT GCC ATG TAG ACC-3′	5′-TTG AGC ACA GGG TAC TTT A-3′
hSTAT1	5′-ACC CAA TCC AGA TGT CTA TG-3′	5′-GAG CCT GAT TAA ATC TCT GG-3′
hIRF1	5′-ATA CCT TCT CTG ATG GAC TC-3′	5′-GAA GTT GTA CAG ATC ACT GG-3′
hIRF9	5′-CTC AGA AAG TAC CAT CAA AGC-3′	5′-TCA TTA TTG AGG GAG TCC TG-3′
hSTAT2	5′-ATA TAA GAT CCA GGG CCA AAG G-3′	5′-CAG TAG CTC GAT TAG GGT AG-3′
hIFN-β	5′-ATT CTA ACT GCA ACC TTT CG-3′	5′-GTT GTA GCT CAT GGA AAG AG-3′

h, human; m, murine.

regulation of IL-27 production in IRAK1–deficient macrophages. Because optimal IL-27 production relies on autocrine IFN-β signaling, we tested the impact of MRT67307 on type I IFN expression, analyzing IFN-β mRNA expression in MRT67307-treated WT and IRAK1$^{-/-}$ BMDM stimulated with LPS and poly(I:C) (Fig. 1D). MRT67307 inhibited TLR3/4-induced IFN-β expression in WT BMDM and in LPS-stimulated IRAK1$^{-/-}$ macrophages. In contrast, we detected high levels of IFN-β in poly(I:C)-stimulated IRAK1$^{-/-}$ compared with WT macrophages (35), which we found to remain high following MRT67307 treatment (Fig. 1D). This means that for TLR3 responses, the second phase in IL27p28 expression involving the IFNAR signaling pathway remains active in MRT67307-treated IRAK1$^{-/-}$ cells, giving understanding to the differences observed between TLR3 and TLR4 responses (Fig. 1C).

We next examined IL-27 at the transcriptional level, measuring p28 and EBI3 subunit expression by quantitative RT-PCR (qRT-PCR) (Table I) in LPS- and poly(I:C)-stimulated WT and IRAK1-deficient macrophages. Supporting our findings from ELISAs, we observed a significant increase in IL-27p28 expression following poly(I:C) and LPS stimulation in IRAK1$^{-/-}$ BMDM compared with WT BMDM [$p < 0.05$, poly(I:C); $p < 0.001$, LPS; Fig. 1E]. EBI3 mRNA levels were increased basally in IRAK1$^{-/-}$ BMDM and increased further, albeit not significantly, following LPS and poly(I:C) stimulation compared with WT macrophages (Fig. 1F). This finding indicates that IRAK1 negatively regulates the EBI3 subunit also in a stimulus-independent manner. In parallel, we assessed whether blocking the kinase activity of TBK1/IKKε influenced IL-27 subunit expression in both WT and IRAK1-deficient macrophages. MRT67307 reduced IL-27p28 subunit

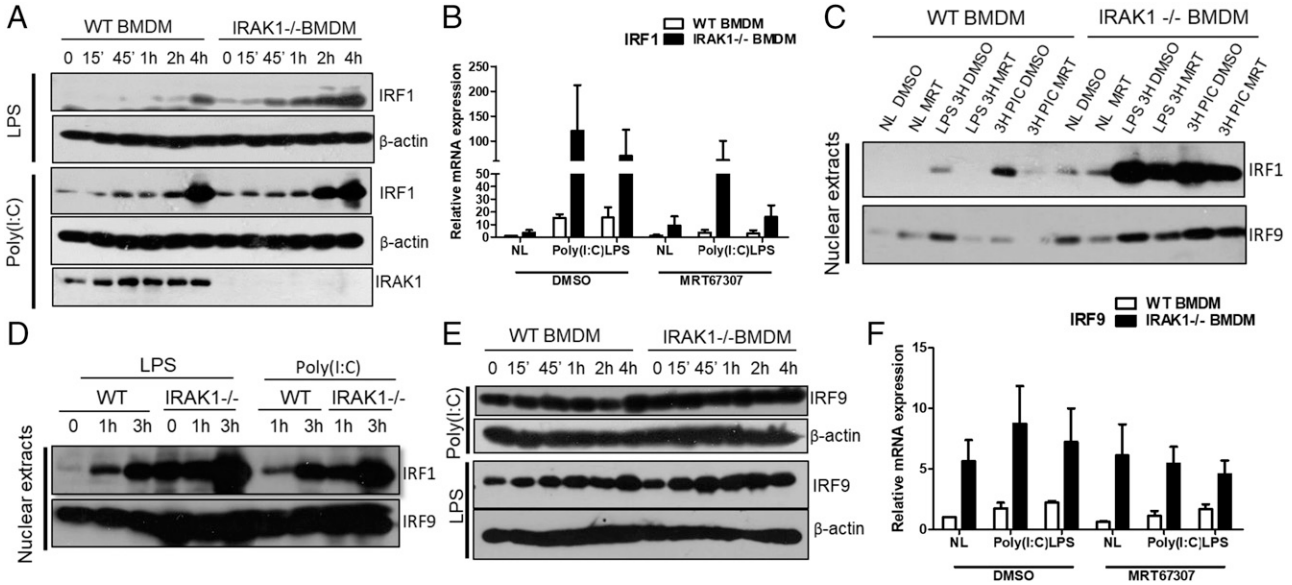

FIGURE 2. IRAK1 regulates IRF1 and IRF9, key transcription factors controlling IL-27p28 expression. (**A** and **E**) WT and IRAK1$^{-/-}$ BMDM were stimulated with poly(I:C) (25 μg/ml) or LPS (1 μg/ml) for the indicated times, and whole cell lysates were generated. Cell lysates were resolved by SDS-PAGE (10%) and subjected to immunoblotting for IRF1, IRF9, and IRAK1, with β-actin as a loading control. Similar results were obtained in two independent experiments. (**B** and **F**) WT and IRAK1$^{-/-}$ BMDM were pretreated with DMSO or MRT67307 (2 μM) for 1.5 h prior to stimulation with 25 μg/ml poly(I:C) or 1 μg/ml LPS for 3 h. Total RNA was isolated and subjected to reverse transcription. IRF1 and IRF9 mRNA were measured by quantitative real time RT-PCR, normalized against GAPDH mRNA, and shown as the mean (±SEM) of three independent experiments performed in triplicate. One-way ANOVA with a post hoc Tukey test was conducted for multiple experimental group comparison. (**C** and **D**) Where indicated, WT and IRAK1$^{-/-}$ BMDM were pretreated with DMSO or MRT67307 (2 μM) for 1.5 h prior to stimulation with 25 μg/ml poly(I:C) or 1 μg/ml LPS for the indicated times, and nuclear lysates were generated. Lysates were subjected to immunoblotting with the indicated Abs. Similar results were obtained in two independent experiments.

expression in WT macrophages stimulated by both LPS (351-fold versus 119-fold; NS) and poly(I:C) (71-fold versus 10-fold; NS) ligands. Pretreatment of IRAK1$^{-/-}$ BMDM with MRT67307 reduced the increase in IL27p28, with a more pronounced reduction observed in LPS-stimulated IRAK1$^{-/-}$ BMDM ($p < 0.001$; Fig. 1E) when compared with poly(I:C) (257-fold versus 117-fold; NS, Fig. 1E), paralleling our findings from ELISAs (Fig. 1C). Pretreating WT or IRAK1$^{-/-}$ BMDM with MRT67307 failed to influence EBI3 mRNA expression at the basal level or following ligand stimulation.

IRAK1 regulates IRF1 and IRF9, key regulators of IL-27p28 expression

Previous studies have shown that IRF1, IRF3, and IRF9 play pivotal roles in IL-27p28 expression downstream of both TLR3 and TLR4 (4). Therefore, we next addressed the role of IRAK1 in the regulation of these transcription factors.

We observed higher protein levels of IRF1 in IRAK1$^{-/-}$ BMDM compared with WT BMDM following both LPS and poly(I:C) ligand stimulation conditions, and this increase in IRF1 was noted at earlier time points in IRAK1-deficient macrophages (Fig. 2A). To determine if this increase in IRF1 protein is reflected at the mRNA level, we examined for differences in mRNA expression levels of IRF1 by qRT-PCR in WT versus IRAK1$^{-/-}$ BMDM following poly(I:C) and LPS stimulation (Fig. 2B). A modest increase in the basal levels of IRF1 mRNA was observed in IRAK1$^{-/-}$ BMDM compared with WT macrophages. However, following ligand stimulation, the observed increase in IRF1 mRNA levels in IRAK1-deficient macrophages was quite marked [120-fold in IRAK1$^{-/-}$ versus 15-fold in WT BMDM following poly(I:C) stimulation and 70-fold in IRAK1$^{-/-}$ versus 15-fold following LPS stimulation; Fig. 2B]. Pretreatment of WT macrophages with MRT67307 reduced TLR4-induced (15-fold versus 3-fold in MRT67307) and TLR3-induced (15-fold versus 4-fold in MRT67307) IRF1 mRNA levels (Fig. 2B). Using MRT67307 in IRAK1$^{-/-}$ BMDM led to a reduction in IRF1 mRNA levels in poly(I:C)-stimulated, IRAK1-deficient macrophages (120-fold versus 62-fold in MRT67307); a more pronounced reduction was seen in LPS-stimulated cells (70-fold versus 16-fold in MRT67307-pretreated IRAK1$^{-/-}$ BMDM) (Fig. 2B). Examining IRF1 regulation further, we observed a marked increase in the nuclear levels of IRF1 in IRAK1$^{-/-}$ macrophages compared with WT macrophages at 3 h post–ligand stimulation (Fig. 2C). In response to LPS, we observed high nuclear levels of IRF1 as early as 1 h post–ligand stimulation in IRAK1$^{-/-}$ macrophages (Fig. 2D). Pretreatment of WT BMDM with MRT67307 led to reduced nuclear levels of IRF1 following LPS and poly(I:C) ligand stimulation conditions (Fig. 2C). Using MRT67307 in the IRAK1$^{-/-}$ BMDM, we observed only a modest reduction in the nuclear levels of IRF1 following poly(I:C) and LPS stimulation. Reduced IRF1 nuclear levels may be explained in part by our findings that MRT67037 leads to a decrease in TLR ligand–induced IRF1 mRNA expression in both WT and IRAK1-deficient macrophages (Fig. 2B).

We have previously shown that hyperactivation of IRF3 occurs in IRAK1$^{-/-}$ compared with WT BMDM following TLR3 activation

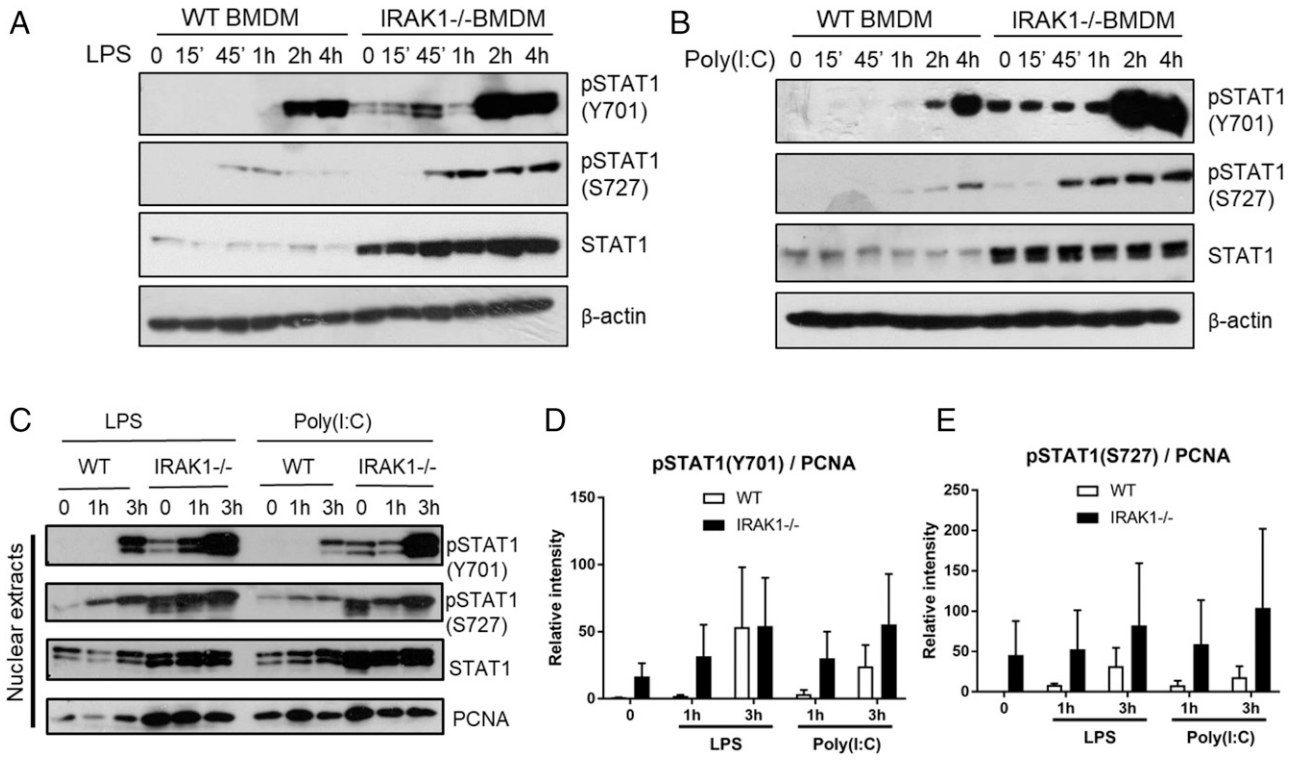

FIGURE 3. IRAK1 regulates STAT1 activation and expression levels following TLR3 and TLR4 stimulation. (**A** and **B**) WT and IRAK1$^{-/-}$ BMDM were stimulated with poly(I:C) (25 μg/ml) or LPS (1 μg/ml) for the indicated times, and whole cell lysates were generated. Cell lysates were resolved by SDS-PAGE (10%) and subjected to immunoblotting for p-STAT1 (Y701), p-STAT1 (S727), and total STAT1, with β-actin as a loading control. Similar results were obtained in three independent experiments. (**C**) WT and IRAK1$^{-/-}$ BMDM were stimulated with 25 μg/ml poly(I:C) or 1 μg/ml LPS for 1 and 3 h, and nuclear lysates were generated. Lysates were subjected to immunoblotting with the indicated Abs. Similar results were obtained in three independent experiments. (**D** and **E**) Relative ratio of phospho-STAT1/PCNA (nuclear loading control) in WT and IRAK1$^{-/-}$ BMDM at 1 and 3 h following poly(I:C) and LPS stimulation, as determined by densitometric analysis of three independent experiments.

(35). In this study, we observed no increase in IRF3 activation in IRAK1$^{-/-}$ BMDM following TLR4 ligand stimulation (Supplemental Fig. 1).

IRF9 is thought to act primarily downstream of IFNAR as part of the ISGF3 complex, influencing the expression of a vast number of IFN-stimulated genes, including IL-27p28 (4, 36). To date, limited data have been published on factors regulating IRF9 or indeed its biological role in TLR signaling (36). We observed increased IRF9 protein levels in IRAK1$^{-/-}$ compared with WT BMDM in unstimulated cells and following poly(I:C) and LPS stimulation (Fig. 2E). Profiling nuclear IRF9 revealed that IRAK1-deficient macrophages consistently showed increased nuclear levels of IRF9 following LPS and poly(I:C) stimulation compared with WT macrophages (Fig. 2C, 2D). MRT67307 had a minimal effect on the high nuclear levels of IRF9 observed in TLR ligand–stimulated IRAK1$^{-/-}$ macrophages (Fig. 2C). Next, we examined whether IRAK1 regulates IRF9 at the transcriptional level. Increased IRF9 mRNA was observed basally and following poly(I:C) and LPS stimulation of IRAK1$^{-/-}$ macrophages compared with WT macrophages (Fig. 2E). Pretreating IRAK1$^{-/-}$ or WT BMDM with MRT67307 failed to influence either basal or ligand-stimulated levels of IRF9 mRNA (Fig. 2F). Taken together, these data reveal that members of the noncanonical IκB kinases TBK1 or IKKε are involved in the transcriptional regulation of IRF1 but not IRF9.

The identification of IRAK1 as a novel regulator of STAT1

STAT1 is critically involved in IL-27p28 gene transcription downstream of IFNAR. Phosphorylation of STAT1 at S727 occurs independently of autocrine IFN signaling for TLR4; in contrast, a dependency on the IFNAR pathway has been speculated but not proven conclusively for TLR3 (37). STAT1 phosphorylation at Y701 downstream of TLR3 and TLR4 is dependent on autocrine type I IFN signaling (37). Increased activation of STAT1 was seen in IRAK1$^{-/-}$ compared with WT macrophages following both LPS and poly(I:C) ligand stimulation conditions (Fig. 3A, 3B). Examining nuclear levels of STAT1, we observed increased levels of p-STAT1 in IRAK1-deficient macrophages compared with WT macrophages and at the earlier time point of 1 h after ligand stimulation (Fig. 3C–E). Further profiling revealed a marked increase in the basal levels of total STAT1 in IRAK1-deficient macrophages (Fig. 3A, 3B). To our knowledge, this represents the first study to show that IRAK1 regulates STAT1 activation downstream of TLRs and furthermore identifies IRAK1 as a novel modulator of STAT1 expression. Examining this finding further, we performed quantitative real-time PCR to assess the relative expression of STAT1 in IRAK1$^{-/-}$ compared with WT macrophages. In unstimulated cells, we observed higher mRNA levels for STAT1 in IRAK1$^{-/-}$ versus WT BMDM, with the same finding observed following stimulation with poly(I:C) and LPS (Fig. 4A). Pretreatment of WT and IRAK1$^{-/-}$ BMDM with MRT67307 reduced STAT1 expression levels following stimulation with poly(I:C) or LPS (Fig. 4A). Next, we stimulated WT and IRAK1$^{-/-}$ macrophages with poly (I:C) and LPS, in the presence or absence of MRT67307, and examined nuclear levels of p-STAT1 (Y701), which is dependent on IFNAR signaling (Fig. 4B). A marked increase in the nuclear levels of p-STAT1 was clearly observed in IRAK1$^{-/-}$ compared with WT macrophages. The heightened nuclear levels of p-STAT1 seen in IRAK1$^{-/-}$ macrophages were greatly reduced by MRT67307 following TLR4 ligand stimulation. In contrast, MRT67307 barely affected p-STAT1 nuclear levels following poly(I:C) stimulation of IRAK1$^{-/-}$ macrophages (Fig. 4B), possibly due to sustained IFN-β production driving STAT1 activation (Fig. 1D).

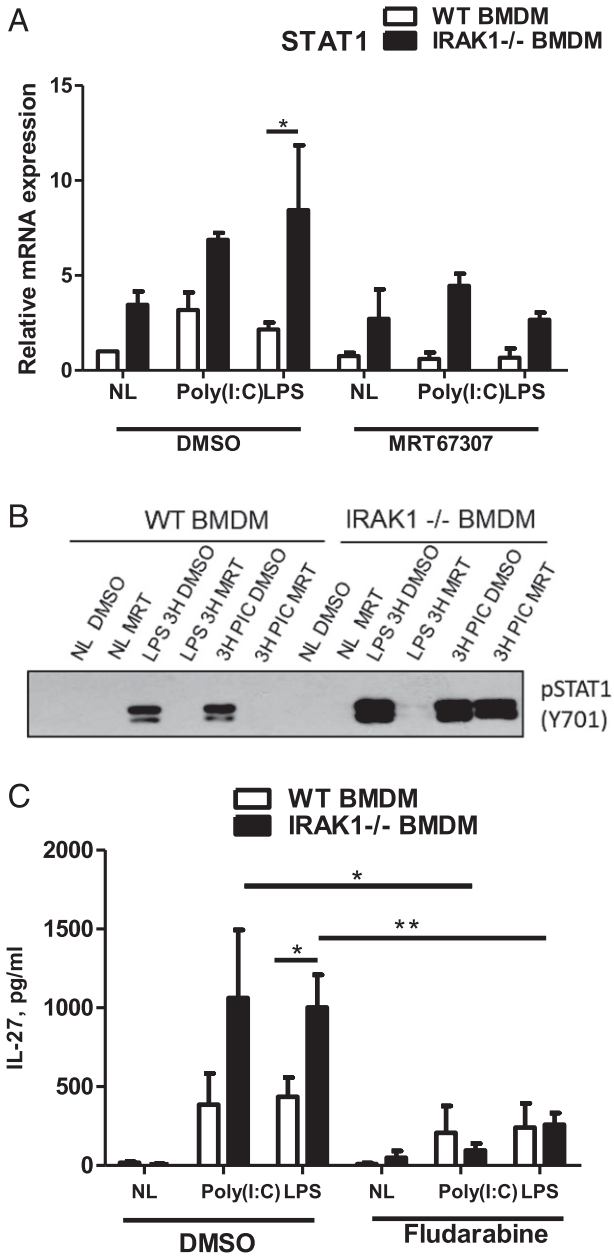

FIGURE 4. (**A**) WT and IRAK1$^{-/-}$ BMDM were pretreated with DMSO or MRT67307 (2 μM) for 1.5 h prior to stimulation with 25 μg/ml poly(I:C) or 1 μg/ml LPS for 3 h. Total RNA was isolated and subjected to reverse transcription. STAT1 mRNA was measured by quantitative real time RT-PCR, normalized against GAPDH mRNA, and shown as the mean (±SEM) of three independent experiments performed in triplicate. One-way ANOVA with a post hoc Tukey test was conducted for multiple experimental group comparison. (**B**) WT and IRAK1$^{-/-}$ BMDM were pretreated with DMSO or MRT67307 (2 μM) for 1.5 h prior to stimulation with 25 μg/ml poly(I:C) or 1 μg/ml LPS for 3 h, and nuclear lysates were generated. Lysates were subjected to immunoblotting with the indicated Abs. Similar results were obtained in three independent experiments. (**C**) STAT1 is required for IL-27 production downstream of both TLR3 and TLR4. WT or IRAK1$^{-/-}$ BMDM were seeded and stimulated for 9 h with 25 μg/ml poly(I:C) or for 6 h with 1 μg/ml LPS. Cells had been pretreated with 50 μM fludarabine (STAT1 inhibitor) or the same volume of DMSO as a vehicle control for 24 h. Supernatants were collected, and IL-27 levels were measured by ELISA. The p values were calculated using the unpaired Student t test. *$p < 0.05$, **$p < 0.01$. NL, no ligand.

Because STAT1 expression together with activity are increased in IRAK1$^{-/-}$ macrophages, we decided to address whether blocking STAT1 could significantly impact the elevated IL-27

levels observed in IRAK1$^{-/-}$ BMDM. Fludarabine, a nucleoside analog, inhibits STAT1, and work has shown that it depletes STAT1 at the mRNA and protein level while not affecting other STAT members (38). Pretreating IRAK1$^{-/-}$ BMDM with fludarabine significantly reduced IL-27 production following LPS ($p < 0.01$) and poly(I:C) ($p < 0.05$) ligand stimulation conditions (Fig. 4C). Altogether, we have uncovered a novel function of IRAK1 in regulating STAT1 expression and activation.

IRAK1 regulates the key transcription factors involved in TLR-induced IL-27 production in a human microglial cell line

We successfully generated stable knockdown for IRAK1 in human microglial cells (CHME3) and used a nontargeting control shRNA for control cells. We found significantly increased IL-27 levels in IRAK1 knockdown cells compared with control cells following LPS and poly(I:C) stimulation [$p < 0.05$, poly(I:C); $p < 0.05$, LPS; Fig. 5A]. Interestingly, we also observed increased basal levels of IL-27 in IRAK1 knockdown cells ($p < 0.01$). Western blot analysis confirmed knockdown of IRAK1 in the microglial cells (~80–90%) used for ELISA (Fig. 5B). Because STAT1 is key to the mechanistic understanding of the observed increase in IL-27, we next profiled IRAK1 knockdown cells compared with control cells by Western blot analysis. LPS- and poly(I:C)-stimulated IRAK1 knockdown cells showed increased activation of STAT1 as well as increased expression of IRF1, IRF9, and STAT1 compared with control cells (Fig. 5C).

IRAK1 regulates IL-27 production downstream of IFNAR

Assessing levels of IL-27 by ELISA in IFN-β–stimulated WT and IRAK1-deficient macrophages revealed a significant increase in IL-27 production in the IRAK1$^{-/-}$ compared with WT macrophages ($p < 0.01$, 6 h; Fig. 6A). We next examined IL-27 at the transcriptional level, measuring p28 and EBI3 subunit expression by qRT-PCR in IFN-β–stimulated control and IRAK1 knockdown human microglial cells (CHME3). We observed an increase in IL-27p28 expression (10-fold versus 3-fold) and EBI3 (6-fold versus 2-fold) following IFN-β stimulation in IRAK1 knockdown compared with control cells (Fig. 6B, 6C). Examining the key transcription factors regulating IL-27p28 expression downstream of IFNAR, we found increased expression of IRF1, IRF9, STAT1, and STAT2 at the basal level as assessed by qRT-PCR (Fig. 6D–G). For IRF1 and IRF9, a marked increase in mRNA expression levels was observed in response to IFN-β in IRAK1 knockdown cells (Fig. 6F, 6G). Type I IFN signaling leads to the formation of ISGF3 and STAT1 homodimers; the latter positively regulates IRF1 gene expression by its binding to the IFN-γ activation site. Our findings prompted us to examine nuclear levels of activated STAT1 in IFN-β–stimulated, IRAK1-deficient macrophages compared with WT macrophages (Fig. 7). We detected increased nuclear levels of p-STAT1, IRF1, and IRF9 in IRAK1-deficient macrophages compared with WT macrophages (Fig. 7). A marked increase in the nuclear levels of IRF1 was observed as early as 1 h after IFN-β stimulation in IRAK1-deficient macrophages (Fig. 7A, 7E). Next, through Western blot analysis of whole cell lysates generated from control and IRAK1 knockdown human microglial cells, we showed increased basal levels of IRF1, IRF9, STAT1, and STAT2 as well as increased IRF1/9 levels following IFN-β stimulation (Fig. 8A). Increased activation of STAT1 was observed in IRAK1 knockdown cells compared with control cells following IFN-β stimulation, whereas we observed less marked differences in the activation profile for STAT2 (Fig. 8A). Examining IFN-β mRNA expression by qRT-PCR showed a significant increase in the basal expression of IFN-β in IRAK1 knockdown cells compared with control cells (Fig. 8B). Blocking the kinase activity of TBK1/IKKε with MRT67307 in IRAK1 knockdown cells

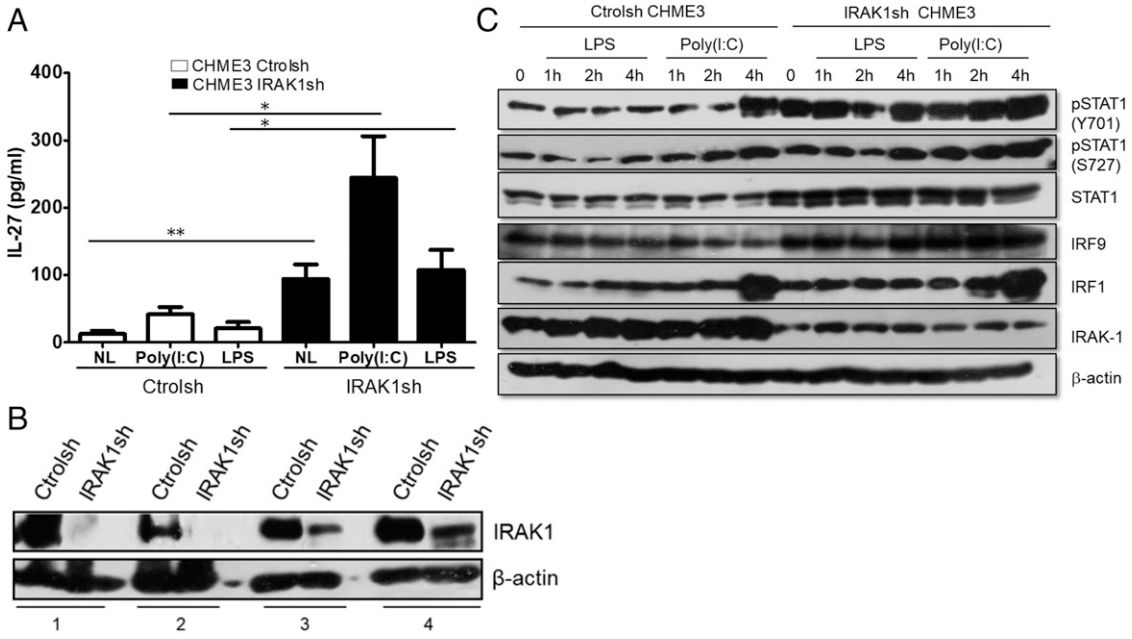

FIGURE 5. IRAK1 regulates the TLR3/4–STAT1–IL-27 signaling in human microglial cells. (**A**) Stable IRAK1 knockdown (IRAK1sh; short-hairpin RNA) and control (Ctrolsh) human microglial cells (CHME3) were stimulated with 25 μg/ml poly(I:C) or 1 μg/ml LPS. Supernatants were collected after 12 h, and IL-27 levels were measured through ELISA. Data are the mean (±SEM) of four independent experiments performed in triplicate. The p values were calculated using the unpaired Student t test. *$p < 0.05$, **$p < 0.01$. (**B**) Lysates were generated from IRAKsh and Ctrolsh wells following supernatant collection for ELISA experiments shown in Fig. 4A, which were subsequently subjected to immunoblotting with IRAK1 and β-actin Abs to validate knockdown of IRAK1. (**C**) IRAKsh and controlsh cells were stimulated with 25 μg/ml poly(I:C) or 1 μg/ml LPS for the indicated times, and whole cell lysates were generated. Cell lysates were resolved by SDS-PAGE (10%) and subjected to immunoblotting with the indicated Abs. Similar results were obtained in three independent experiments. NL, no ligand.

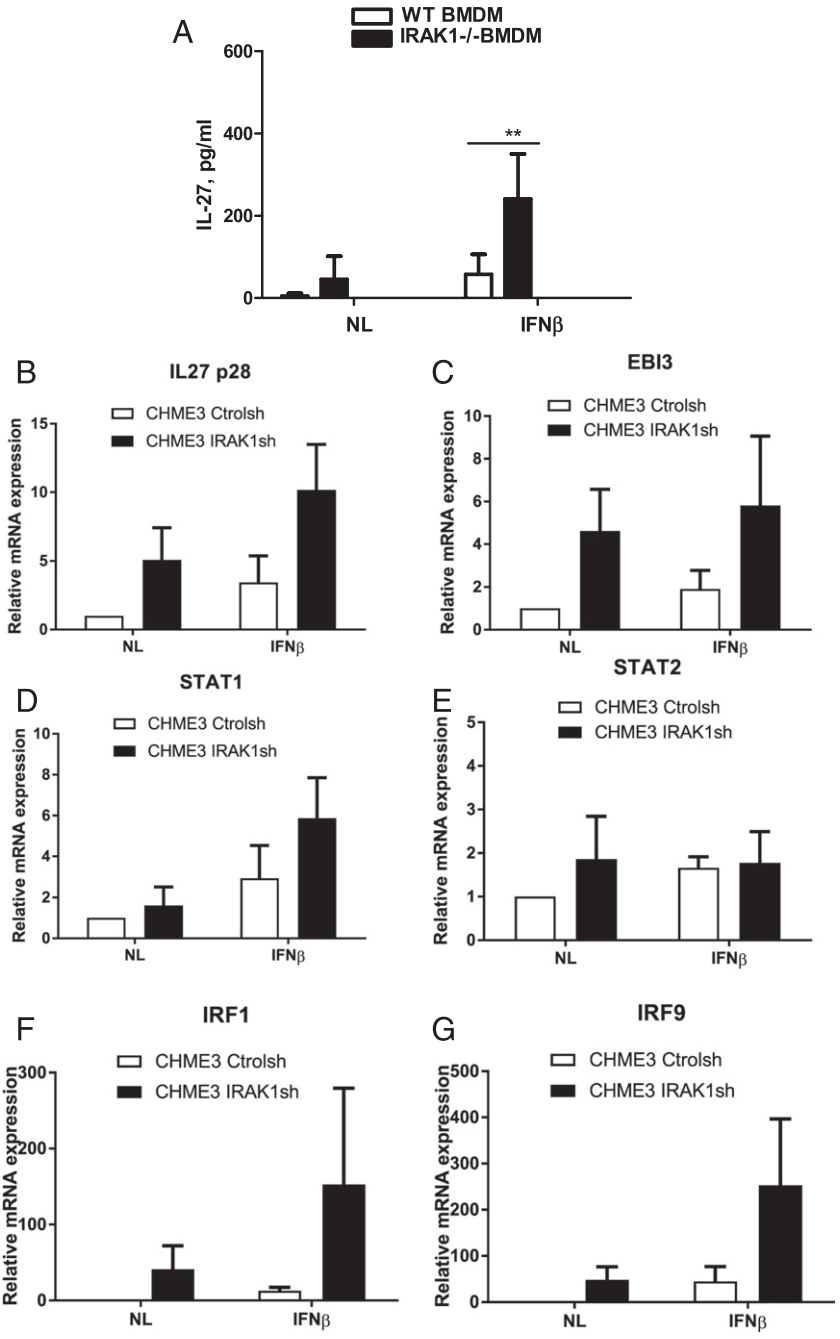

FIGURE 6. IRAK1 regulates IL-27 production downstream of IFNAR. (**A**) WT and IRAK$^{-/-}$ BMDM were seeded at a concentration of 1×10^6 cells/ml and treated the following day with 10 ng/ml murine IFN-β or no ligand (NL) for 8 h. Cell supernatants were then collected, and IL-27 concentration was measured by ELISA. The mean ± SD of six independent experiments, performed in triplicate, is shown. The p values were calculated using the unpaired Student t test. $^{**}p < 0.01$. (**B**–**G**) Stable IRAK1 knockdown (IRAK1sh; short-hairpin RNA) and control (Ctrolsh) human microglial cells (CHME3) were seeded at 5×10^5 cells/ml and treated the next day with NL and 10 ng/ml of human IFN-β for 2 h. Total RNA was isolated and subjected to qRT-PCR for the indicated targets, normalized against GAPDH mRNA, and shown as the mean (±SEM) of four independent experiments performed in triplicate.

reduced STAT1/2 protein levels as assessed by Western blot analysis (Fig. 8C–E). These results prompted us to profile STAT1 expression and activation by immunoblot analysis in TBK1-deficient macrophages. We observed reduced activation and expression levels of STAT1 in LPS and poly(I:C) ligand–stimulated TBK1$^{-/-}$ macrophages compared with their control counterpart cells (Fig. 9A, 9B). We also observed a slight reduction in total STAT2 levels in TBK1-deficient macrophages compared with control cells (Fig. 9A, 9C). Not surprisingly, TBK1-deficient macrophages showed impaired IL-27 cytokine production compared with control BMDM following LPS ($p < 0.01$, 6 h) and poly(I:C) ($p < 0.05$, 6 h) ligand stimulation conditions (Fig. 9D).

Discussion

We reported previously that IRAK1 limits TLR3-induced IFN-β production (35), whereas LPS-stimulated, IRAK1-deficient macrophages showed comparable IFN-β levels to control cells (35). In contrast to these findings for IFN-β, IRAK1 limits TLR3- and TLR4-induced IL-27 production. Knowledge that IRF3 is an important transcriptional regulator of IL-27p28 expression prompted us to examine whether TBK1, the IRF3-activating kinase, played a significant role in TLR3/4-driven IL-27 production. Pretreating WT macrophages with a dual TBK1/IKKε kinase inhibitor significantly reduced both LPS- and poly(I:C)-induced IL-27p28 expression and IL-27 cytokine levels. In contrast to IL-27p28 subunit expression, blocking TBK1/IKKε kinase activity failed to influence ligand-induced EBI3 subunit expression under the same stimulation conditions. IRAK1-deficient macrophages showed increased expression of EBI3 mRNA following LPS and poly(I:C) stimulation, most notably following LPS stimulation. This points to the hyperactivation of an NF-κB–independent mechanism regulating EBI3 expression

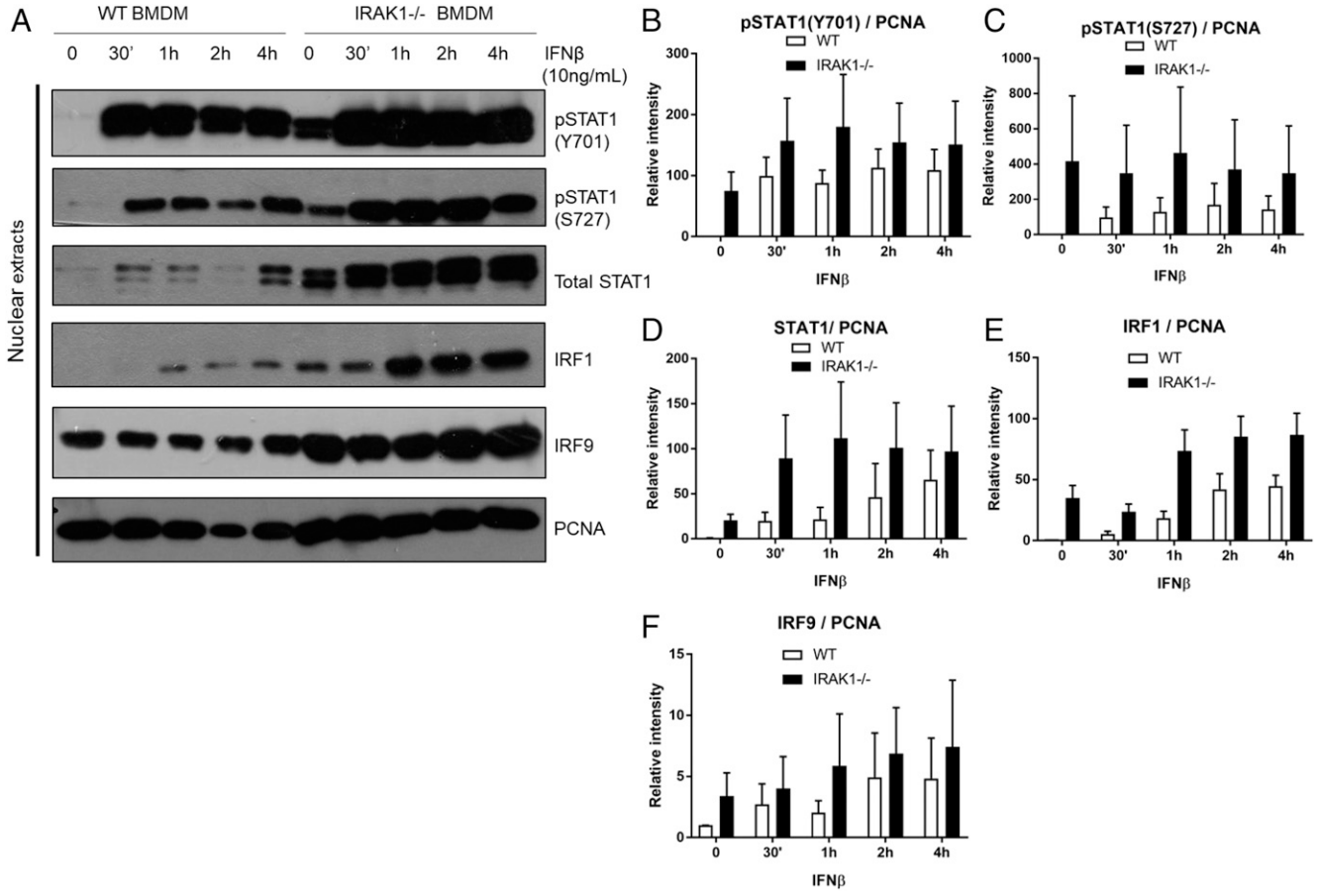

FIGURE 7. (**A**) WT and IRAK1$^{-/-}$ BMDM were stimulated with mIFN-β (10 ng/ml) for the indicated time points, and nuclear lysates were generated. Lysates were subjected to immunoblotting with the indicated Abs. Similar results were obtained in three independent experiments. (**B**) Relative ratio of p-STAT1(Y701)/PCNA (nuclear loading control), (**C**) p-STAT1(S727)/PCNA, (**D**) total STAT1/PCNA, (**E**) IRF1/PCNA, and (**F**) IRF9/PCNA in WT and IRAK1$^{-/-}$ BMDM following mIFN-β stimulation, as determined by densitometric analysis of three independent experiments.

because IRAK1 deficiency reduces NF-κB activation following LPS stimulation.

Focusing on how IL-27p28 expression is regulated, we investigated whether deregulated expression/activity of IRF1/3/9 accounted for higher TLR stimulus-driven IL-27p28 expression observed in IRAK1-deficient macrophages. We observed earlier induction and higher expression levels of IRF1, including pronounced nuclear levels, following LPS and poly(I:C) stimulation in IRAK1-deficient macrophages compared with control cells. TLR4-induced expression and activation of IRF1 is dependent on MyD88 (31), whereas TLR3-induced activation of IRF1 is presumed to rely on autocrine IFN-β signaling (2). Previous work has shown a positive role for IRF1 in the early phase of LPS-induced IL-27p28 gene expression (2-h time point) and a later phase downstream of IFNAR following LPS and poly(I:C) ligand stimulation (2). STAT1 is known to regulate IRF1 expression (39), which most likely contributes to the increase in IRF1 levels observed following LPS, poly(I:C), and IFN-β stimulation in IRAK1-deficient macrophages, which show hyperactivation of STAT1.

TLR3/4-stimulation led to pronounced nuclear levels of IRF9 in IRAK1-deficient macrophages compared with control cells accompanied by increased expression at the mRNA and protein level in unstimulated cells. Work using IRF9-deficient dendritic cells has previously defined a crucial role for IRF9 in poly(I:C)-driven early and late phase IL-27p28 expression, whereas a dependency on late phase p28 expression was reported for IRF9 downstream of TLR4 (4). Most certainly, the observed increase in IRF9 contributes to the heightened levels of TLR3/4 stimulus-driven IL-27 in IRAK1-deficient macrophages. IRF9 expression is regulated by STAT1 and IRF1 (39), which may explain the increase observed in IRAK1-deficient cells.

Interestingly, this work has unfolded a novel regulatory role for IRAK1 in STAT1 activation. Previous studies determined a requirement for the scaffold function of IRAK1 in IL-1–induced S727 phosphorylation of STAT1 (40). In contrast to IL-1R signaling, we report hyperactivation of STAT1 (S727) following LPS and poly(I:C) stimulation in both murine and human IRAK1-deficient immune cells. In TLR4 signaling, phosphorylation of STAT1 at S727 is dependent on MyD88 and TRIF signaling but independent of IRF3, IRF7, and IFNAR (37). Recent work highlighted a role for STAT1 (S727) in the regulation of TNF-α production downstream of several TLRs, including TLR4, but to date, knowledge of TLR-specific, STAT1-regulated genes is limited (37).

TLR-induced activation of STAT1 at Y701 is considered IFNAR signaling dependent (37). In IRAK1-deficient macrophages, TLR-induced STAT1 hyperphosphorylation (Y701) prompted us to examine whether IRAK1 could be controlling IL-27 expression beyond the TLR-specific phase. Stimulating IRAK1-deficient macrophages with IFN-β led to heightened IL-27 cytokine levels accompanied by increased nuclear levels of p-STAT1 and IRF1 compared with control macrophages. To our knowledge, this work

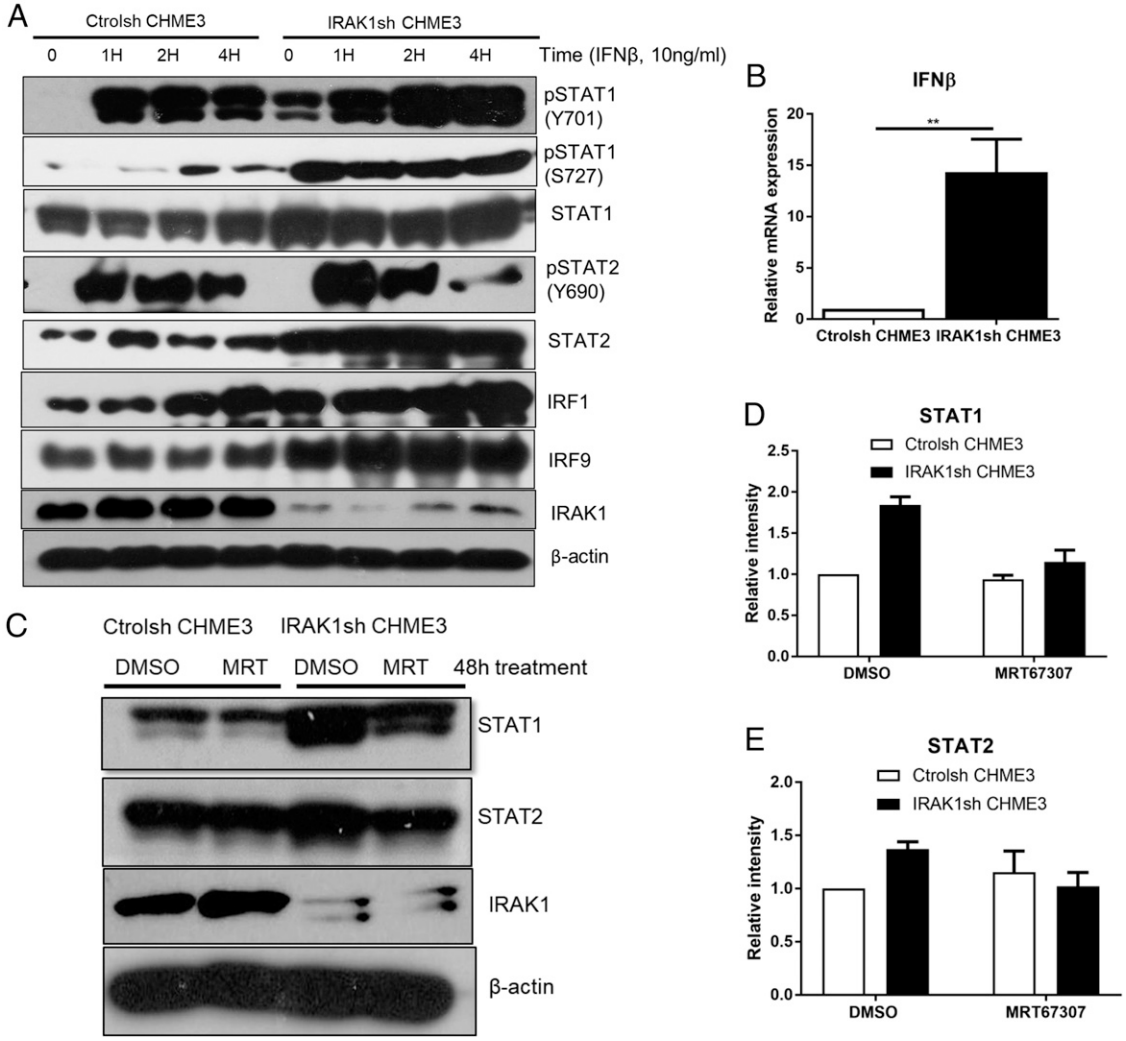

FIGURE 8. IRAK1 is involved in the regulation of the STAT-IRF signaling axis downstream of IFNAR. (**A**) Stable IRAK1 knockdown (IRAK1sh; short-hairpin RNA) and control (Ctrolsh) human microglial cells (CHME3) were seeded at a density of 5×10^5 cells/ml. The next day, the cells were stimulated with IFN-β (10 ng/ml) and harvested at the indicated times (0–4 h). The resulting lysates were resolved by SDS-PAGE (10%) and subjected to immunoblotting for p-STAT1 (Y701), p-STAT1 (S727), total STAT1, p-STAT2 (Y690), total STAT2, IRF1, IRF9, and IRAK1, with β-actin as a loading control. Similar results were obtained in three independent experiments. (**B**) CHME3 Ctrolsh and IRAK1sh cells were seeded at 5×10^5 cells/ml, and the next day, total RNA was isolated and subjected to qRT-PCR for IFN-β, normalized against GAPDH mRNA, and shown as the mean (±SEM) of five independent experiments performed in triplicate. The *p* values were calculated using the unpaired Student *t* test. $^{**}p < 0.01$. (**C**) IRAKsh and controlsh cells were treated with MRT67307 (2 μM) for 48 h, and whole cell lysates were generated. Cell lysates were resolved by SDS-PAGE and subjected to immunoblotting with the indicated Abs. Similar results were obtained in three independent experiments. (**D** and **E**) Relative ratio of total STAT1/β-actin and total STAT2/β-actin in DMSO- and MRT67307-treated IRAKsh and controlsh cells, as determined by densitometric analysis of three independent experiments.

provides the first evidence that IRAK1 acts downstream of IFNAR, regulating the activity of STAT1 and, consequently, the expression of STAT1 target genes. IRAK1 may be involved in the regulation of phosphatases or kinases controlling STAT1 activation downstream of both TLR and IFNAR signaling pathways.

We found that IRAK1 controls the basal levels of STAT family members STAT1 and STAT2. We detected higher mRNA and protein levels of STAT1 and STAT2 in IRAK1 knockdown compared with control cells. Previous work has shown that STAT1 protein levels are reduced in dendritic cells isolated from catalytically inactive IRAK1 (D359) mice (41). Considering these data, we may suggest that the scaffold and kinase function of IRAK1 are both required to maintain normal basal levels of STAT1. Low-level IFN-β signaling is required to maintain adequate levels of STAT1 and its target genes, as evidenced by diminished STAT1 protein levels observed in IFNAR, IRF3, TRIF, and TRAM-deficient macrophages (42–44). In earlier work, we observed hyperactivation of TBK1 in unstimulated, IRAK1-deficient macrophages (35). We speculate that hyperactivated TBK1 may contribute to the observed increase in STAT1/2 protein levels by supporting an increase in autocrine IFN-β signaling, driving IRF1 expression, a known transcriptional regulator of STAT1 and STAT2 (39). Supporting this possibility, we observed an increase in IFN-β and IRF1 mRNA levels in unstimulated IRAK1 knockdown cells compared with control cells. Indeed, treating IRAK1-deficient microglial cells with a TBK1/IKKε kinase inhibitor almost reduced STAT1/2 protein to levels observed in control cells. Furthermore, TBK1-deficient macrophages showed reduced levels of STAT1 and STAT2, supporting our idea that TBK1 is actively involved in the maintenance of autocrine IFN-β signaling in cells. IRAK1 may additionally participate in the regulation of STAT1 expression at the posttranslational level, perhaps by controlling the activity of E3 ubiquitin ligases. Several have already been functionally

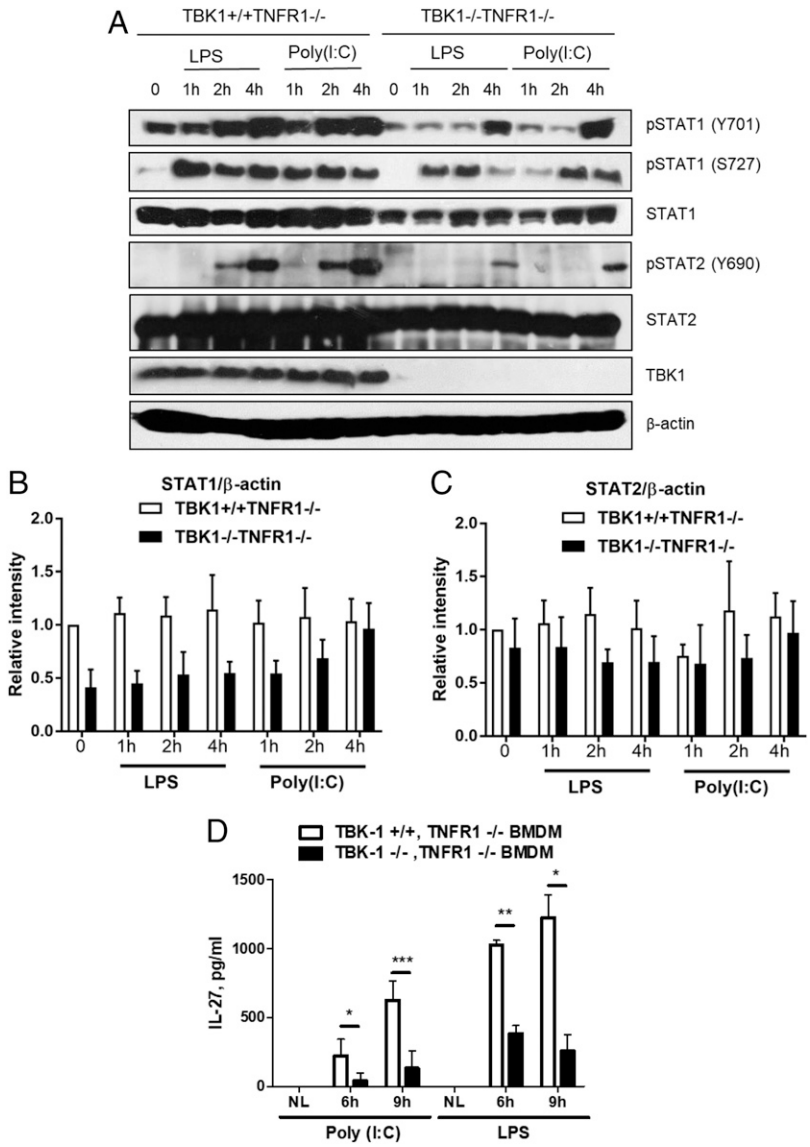

FIGURE 9. TBK1 is a positive regulator of TLR-induced IL-27 production. (**A**) Reduced STAT1 protein levels in the absence of TBK1. TBK1$^{-/-}$TNFR1$^{-/-}$ BMDM and the control cell line TBK1$^{+/+}$TNFR1$^{-/-}$ BMDM were stimulated with 25 μg/ml poly(I:C) or 1 μg/ml LPS for a series of time points and then harvested. Whole cell lysates were subjected to immunoblotting with the indicated Abs. Similar results were obtained in three independent experiments. (**B** and **C**) Relative ratio of total STAT1/β-actin and total STAT2/β-actin in TBK1$^{+/+}$TNFR1$^{-/-}$ and TBK1$^{-/-}$TNFR1$^{-/-}$ BMDM, as determined by densitometric analysis of three independent experiments. (**D**) TBK1 is a positive regulator of IL-27 production downstream of TLR4 and TLR4. TBK1-deficient TBK1$^{-/-}$TNFR1$^{-/-}$ BMDM and the control cell line TBK1$^{+/+}$TNFR1$^{-/-}$ were seeded in parallel and left overnight. The following day, cells were treated with 25 μg/ml poly(I:C) or 1 μg/ml LPS for the indicated time points. The medium was collected, and IL-27 was measured by ELISA. Data are the mean (±SEM) of three independent experiments performed in triplicates. The p values were calculated using the unpaired Student t test. $*p < 0.05$, $**p < 0.01$, $***p < 0.001$.

linked to STAT1 expression, including SLIM, Smurf1, and c-Cbl (45–47).

In conclusion, we have identified IRAK1 as a novel regulator of STAT1 expression and activation downstream of TLR and IFNAR signaling pathways. We speculate that increased STAT1/2 expression found in IRAK1-deficient cells is driven by highly constitutive IFN-β signaling mediated by hyperactive TBK1. Future work will address exactly how IRAK1 regulates the activation of STAT1 in these pathways and whether this regulation is kinase dependent. Overall, this study uncovers mechanistic details about the complex regulation of IL-27, a key immunomodulatory cytokine of relevance to cancer and autoimmune diseases.

Disclosures

The authors have no financial conflicts of interest.

References

1. Pflanz, S., J. C. Timans, J. Cheung, R. Rosales, H. Kanzler, J. Gilbert, L. Hibbert, T. Churakova, M. Travis, E. Vaisberg, et al. 2002. IL-27, a heterodimeric cytokine composed of EBI3 and p28 protein, induces proliferation of naive CD4+ T cells. *Immunity* 16: 779–790.
2. Molle, C., M. Nguyen, V. Flamand, J. Renneson, F. Trottein, D. De Wit, F. Willems, M. Goldman, and S. Goriely. 2007. IL-27 synthesis induced by TLR ligation critically depends on IFN regulatory factor 3. *J. Immunol.* 178: 7607–7615.
3. Villarino, A. V., and C. A. Hunter. 2004. Biology of recently discovered cytokines: discerning the pro- and anti-inflammatory properties of interleukin-27. *Arthritis Res. Ther.* 6: 225–233.
4. Molle, C., M. Goldman, and S. Goriely. 2010. Critical role of the IFN-stimulated gene factor 3 complex in TLR-mediated IL-27p28 gene expression revealing a two-step activation process. *J. Immunol.* 184: 1784–1792.
5. Jankowski, M., P. Kopiński, and A. Goc. 2010. Interleukin-27: biological properties and clinical application. *Arch. Immunol. Ther. Exp. (Warsz.)* 58: 417–425.
6. Yoshimura, T., A. Takeda, S. Hamano, Y. Miyazaki, I. Kinjyo, T. Ishibashi, A. Yoshimura, and H. Yoshida. 2006. Two-sided roles of IL-27: induction of Th1 differentiation on naive CD4+ T cells versus suppression of proinflammatory cytokine production including IL-23-induced IL-17 on activated CD4+ T cells partially through STAT3-dependent mechanism. *J. Immunol.* 177: 5377–5385.
7. Yoshimoto, T., T. Yoshimoto, K. Yasuda, J. Mizuguchi, and K. Nakanishi. 2007. IL-27 suppresses Th2 cell development and Th2 cytokines production from polarized Th2 cells: a novel therapeutic way for Th2-mediated allergic inflammation. *J. Immunol.* 179: 4415–4423.
8. Neufert, C., C. Becker, S. Wirtz, M. C. Fantini, B. Weigmann, P. R. Galle, and M. F. Neurath. 2007. IL-27 controls the development of inducible regulatory T cells and Th17 cells via differential effects on STAT1. *Eur. J. Immunol.* 37: 1809–1816.
9. Lucas, S., N. Ghilardi, J. Li, and F. J. de Sauvage. 2003. IL-27 regulates IL-12 responsiveness of naive CD4+ T cells through Stat1-dependent and -independent mechanisms. *Proc. Natl. Acad. Sci. USA* 100: 15047–15052.
10. Takeda, A., S. Hamano, A. Yamanaka, T. Hanada, T. Ishibashi, T. W. Mak, A. Yoshimura, and H. Yoshida. 2003. Cutting edge: role of IL-27/WSX-1

signaling for induction of T-bet through activation of STAT1 during initial Th1 commitment. *J. Immunol.* 170: 4886–4890.
11. Pot, C., H. Jin, A. Awasthi, S. M. Liu, C. Y. Lai, R. Madan, A. H. Sharpe, C. L. Karp, S. C. Miaw, I. C. Ho, and V. K. Kuchroo. 2009. Cutting edge: IL-27 induces the transcription factor c-Maf, cytokine IL-21, and the costimulatory receptor ICOS that coordinately act together to promote differentiation of IL-10-producing Tr1 cells. *J. Immunol.* 183: 797–801.
12. Chihara, N., A. Madi, K. Karwacz, A. Awasthi, and V. K. Kuchroo. 2016. Differentiation and characterization of Tr1 cells. *Curr. Protoc. Immunol.* 113: 3.27.1–3.27.10.
13. Pot, C., L. Apetoh, A. Awasthi, and V. K. Kuchroo. 2011. Induction of regulatory Tr1 cells and inhibition of T(H)17 cells by IL-27. *Semin. Immunol.* 23: 438–445.
14. Fitzgerald, D. C., G. X. Zhang, M. El-Behi, Z. Fonseca-Kelly, H. Li, S. Yu, C. J. Saris, B. Gran, B. Ciric, and A. Rostami. 2007. Suppression of autoimmune inflammation of the central nervous system by interleukin 10 secreted by interleukin 27-stimulated T cells. [Published erratum appears in 2008 *Nat. Immunol.* 9: 105.] *Nat. Immunol.* 8: 1372–1379.
15. Fitzgerald, D. C., Z. Fonseca-Kelly, M. L. Cullimore, P. Safabakhsh, C. J. Saris, G. X. Zhang, and A. Rostami. 2013. Independent and interdependent immunoregulatory effects of IL-27, IFN-β, and IL-10 in the suppression of human Th17 cells and murine experimental autoimmune encephalomyelitis. *J. Immunol.* 190: 3225–3234.
16. Fitzgerald, D. C., B. Ciric, T. Touil, H. Harle, J. Grammatikopolou, J. Das Sarma, B. Gran, G. X. Zhang, and A. Rostami. 2007. Suppressive effect of IL-27 on encephalitogenic Th17 cells and the effector phase of experimental autoimmune encephalomyelitis. *J. Immunol.* 179: 3268–3275.
17. Pickens, S. R., N. D. Chamberlain, M. V. Volin, A. M. Mandelin, II, H. Agrawal, M. Matsui, T. Yoshimoto, and S. Shahrara. 2011. Local expression of interleukin-27 ameliorates collagen-induced arthritis. *Arthritis Rheum.* 63: 2289–2298.
18. Moraes, A. S., R. F. Paula, F. Pradella, M. P. Santos, E. C. Oliveira, F. von Glehn, D. S. Camilo, H. Ceragioli, A. Peterlevitz, V. Baranauskas, et al. 2013. The suppressive effect of IL-27 on encephalitogenic Th17 cells induced by multi-walled carbon nanotubes reduces the severity of experimental autoimmune encephalomyelitis. *CNS Neurosci. Ther.* 19: 682–687.
19. Tanida, S., H. Yoshitomi, M. Ishikawa, T. Kasahara, K. Murata, H. Shibuya, H. Ito, and T. Nakamura. 2011. IL-27-producing CD14(+) cells infiltrate inflamed joints of rheumatoid arthritis and regulate inflammation and chemotactic migration. *Cytokine* 55: 237–244.
20. Tang, S. C., X. H. Fan, Q. M. Pan, Q. S. Sun, and Y. Liu. 2015. Decreased expression of IL-27 and its correlation with Th1 and Th17 cells in progressive multiple sclerosis. *J. Neurol. Sci.* 348: 174–180.
21. Babaloo, Z., R. K. Yeganeh, M. Farhoodi, B. Baradaran, M. Bonyadi, and L. Aghebati. 2013. Increased IL-17A but decreased IL-27 serum levels in patients with multiple sclerosis. *Iran. J. Immunol.* 10: 47–54.
22. Hasheminia, S. J., S. Tolouei, S. H. Zarkesh-Esfahani, V. Shaygannejad, H. A. Shirzad, R. Torabi, and M. Hashem Zadeh Chaloshtory. 2015. Cytokines gene expression in newly diagnosed multiple sclerosis patients. *Iran. J. Allergy Asthma Immunol.* 14: 208–216.
23. Liu, L., S. Wang, B. Shan, L. Shao, A. Sato, K. Kawamura, Q. Li, G. Ma, and M. Tagawa. 2008. IL-27-mediated activation of natural killer cells and inflammation produced antitumour effects for human oesophageal carcinoma cells. *Scand. J. Immunol.* 68: 22–29.
24. Matsui, M., T. Kishida, H. Nakano, K. Yoshimoto, M. Shin-Ya, T. Shimada, S. Nakai, J. Imanishi, T. Yoshimoto, Y. Hisa, and O. Mazda. 2009. Interleukin-27 activates natural killer cells and suppresses NK-resistant head and neck squamous cell carcinoma through inducing antibody-dependent cellular cytotoxicity. *Cancer Res.* 69: 2523–2530.
25. Salcedo, R., J. K. Stauffer, E. Lincoln, T. C. Back, J. A. Hixon, C. Hahn, K. Shafer-Weaver, A. Malyguine, R. Kastelein, and J. M. Wigginton. 2004. IL-27 mediates complete regression of orthotopic primary and metastatic murine neuroblastoma tumors: role for CD8+ T cells. *J. Immunol.* 173: 7170–7182.
26. Hisada, M., S. Kamiya, K. Fujita, M. L. Belladonna, T. Aoki, Y. Koyanagi, J. Mizuguchi, and T. Yoshimoto. 2004. Potent antitumor activity of interleukin-27. *Cancer Res.* 64: 1152–1156.
27. Salcedo, R., J. A. Hixon, J. K. Stauffer, R. Jalah, A. D. Brooks, T. Khan, R. M. Dai, L. Scheetz, E. Lincoln, T. C. Back, et al. 2009. Immunologic and therapeutic synergy of IL-27 and IL-2: enhancement of T cell sensitization, tumor-specific CTL reactivity and complete regression of disseminated neuroblastoma metastases in the liver and bone marrow. *J. Immunol.* 182: 4328–4338.
28. Schneider, R., T. Yaneva, D. Beauseigle, L. El-Khoury, and N. Arbour. 2011. IL-27 increases the proliferation and effector functions of human naïve CD8+ T lymphocytes and promotes their development into Tc1 cells. *Eur. J. Immunol.* 41: 47–59.
29. Wirtz, S., C. Becker, M. C. Fantini, E. E. Nieuwenhuis, I. Tubbe, P. R. Galle, H. J. Schild, M. Birkenbach, R. S. Blumberg, and M. F. Neurath. 2005. EBV-induced gene 3 transcription is induced by TLR signaling in primary dendritic cells via NF-kappa B activation. *J. Immunol.* 174: 2814–2824.
30. Liu, J., X. Guan, and X. Ma. 2007. Regulation of IL-27 p28 gene expression in macrophages through MyD88- and interferon-gamma-mediated pathways. *J. Exp. Med.* 204: 141–152.
31. Negishi, H., Y. Fujita, H. Yanai, S. Sakaguchi, X. Ouyang, M. Shinohara, H. Takayanagi, Y. Ohba, T. Taniguchi, and K. Honda. 2006. Evidence for licensing of IFN-gamma-induced IFN regulatory factor 1 transcription factor by MyD88 in Toll-like receptor-dependent gene induction program. *Proc. Natl. Acad. Sci. USA* 103: 15136–15141.
32. Schmitz, F., A. Heit, S. Guggemoos, A. Krug, J. Mages, M. Schiemann, H. Adler, I. Drexler, T. Haas, R. Lang, and H. Wagner. 2007. Interferon-regulatory-factor 1 controls Toll-like receptor 9-mediated IFN-beta production in myeloid dendritic cells. *Eur. J. Immunol.* 37: 315–327.
33. Zhang, J., X. Qian, H. Ning, J. Yang, H. Xiong, and J. Liu. 2010. Activation of IL-27 p28 gene transcription by interferon regulatory factor 8 in cooperation with interferon regulatory factor 1. *J. Biol. Chem.* 285: 21269–21281.
34. Pirhonen, J., J. Sirén, I. Julkunen, and S. Matikainen. 2007. IFN-alpha regulates Toll-like receptor-mediated IL-27 gene expression in human macrophages. *J. Leukoc. Biol.* 82: 1185–1192.
35. Bruni, D., J. Sebastia, S. Dunne, M. Schröder, and M. P. Butler. 2013. A novel IRAK1-IKKε signaling axis limits the activation of TAK1-IKKβ downstream of TLR3. *J. Immunol.* 190: 2844–2856.
36. Suprunenko, T., and M. J. Hofer. 2016. The emerging role of interferon regulatory factor 9 in the antiviral host response and beyond. *Cytokine Growth Factor Rev.* 29: 35–43.
37. Luu, K., C. J. Greenhill, A. Majoros, T. Decker, B. J. Jenkins, and A. Mansell. 2014. STAT1 plays a role in TLR signal transduction and inflammatory responses. *Immunol. Cell Biol.* 92: 761–769.
38. Frank, D. A., S. Mahajan, and J. Ritz. 1999. Fludarabine-induced immunosuppression is associated with inhibition of STAT1 signaling. *Nat. Med.* 5: 444–447.
39. Wong, L. H., H. Sim, M. Chatterjee-Kishore, I. Hatzinisiriou, R. J. Devenish, G. Stark, and S. J. Ralph. 2002. Isolation and characterization of a human STAT1 gene regulatory element. Inducibility by interferon (IFN) types I and II and role of IFN regulatory factor-1. *J. Biol. Chem.* 277: 19408–19417.
40. Nguyen, H., M. Chatterjee-Kishore, Z. Jiang, Y. Qing, C. V. Ramana, J. Bayes, M. Commane, X. Li, and G. R. Stark. 2003. IRAK-dependent phosphorylation of Stat1 on serine 727 in response to interleukin-1 and effects on gene expression. *J. Interferon Cytokine Res.* 23: 183–192.
41. Pauls, E., S. K. Nanda, H. Smith, R. Toth, J. S. C. Arthur, and P. Cohen. 2013. Two phases of inflammatory mediator production defined by the study of IRAK2 and IRAK1 knock-in mice. *J. Immunol.* 191: 2717–2730.
42. Fleetwood, A. J., H. Dinh, A. D. Cook, P. J. Hertzog, and J. A. Hamilton. 2009. GM-CSF- and M-CSF-dependent macrophage phenotypes display differential dependence on type I interferon signaling. *J. Leukoc. Biol.* 86: 411–421.
43. Gough, D. J., N. L. Messina, L. Hii, J. A. Gould, K. Sabapathy, A. P. Robertson, J. A. Trapani, D. E. Levy, P. J. Hertzog, C. J. Clarke, and R. W. Johnstone. 2010. Functional crosstalk between type I and II interferon through the regulated expression of STAT1. *PLoS Biol.* 8: e1000361.
44. Stockinger, S., B. Reutterer, B. Schaljo, C. Schellack, S. Brunner, T. Materna, M. Yamamoto, S. Akira, T. Taniguchi, P. J. Murray, et al. 2004. IFN regulatory factor 3-dependent induction of type I IFNs by intracellular bacteria is mediated by a TLR- and Nod2-independent mechanism. *J. Immunol.* 173: 7416–7425.
45. Tanaka, T., M. A. Soriano, and M. J. Grusby. 2005. SLIM is a nuclear ubiquitin E3 ligase that negatively regulates STAT signaling. *Immunity* 22: 729–736.
46. Yuan, C., J. Qi, X. Zhao, and C. Gao. 2012. Smurf1 protein negatively regulates interferon-γ signaling through promoting STAT1 protein ubiquitination and degradation. *J. Biol. Chem.* 287: 17006–17015.
47. Blesofsky, W. A., K. Mowen, R. M. Arduini, D. P. Baker, M. A. Murphy, D. D. Bowtell, and M. David. 2001. Regulation of STAT protein synthesis by c-Cbl. *Oncogene* 20: 7326–7333.